

Quantitative prediction of the freak wave occurrence probability in co-propagating mixed waves

Lei Wang^{a,b}, Kanglixu Ding^a, Binzhen Zhou^{a,*}, Jinxuan Li^b, Shuxue Liu^b, Tianning Tang^c

^a *School of Civil Engineering and Transportation, South China University of Technology, Guangzhou 510641, China*

^b *State Key Laboratory of Coastal and Offshore Engineering, Dalian University of Technology, Dalian 116024, China*

^c *Department of Engineering Science, University of Oxford, Oxford, OX1 3PJ, United Kingdom*

Abstract

The bimodal sea state, which occupies around 15%-25% of the unidirectional sea states suggested in the critical operational environment, is one of the harshest wave conditions in the field of ocean engineering. Quantitative prediction of the freak wave occurrence probability in such co-propagating mixed wave environments is crucial for marine structure designs. Based on our previous study of statistics of long-crested extreme waves, here the quantitative relation between the occurrence probability of freak waves and sea-state parameters is further investigated under bimodal spectral sea-states with equivalent energy but different energy distribution in the frequency band. Unlike the unimodal sea states, the nonlinear interaction process of the co-propagating mixed waves is challenging to theoretically obtain the maximum kurtosis versus their characteristics. In this study, we develop the relation of the maximum kurtosis between single-peak and bimodal wave trains by introducing energy distribution and frequency separation with an empirical formula. A quantitative relation between the occurrence probability of freak waves and kurtosis in co-propagating mixed waves is obtained. It enables the fast and accurate prediction of the occurrence probability of freak waves in the operational area for a given bimodal sea state. This work provides a conservative reference threshold for offshore engineering and ship navigation, as well as ideas and methods for seeking a universal result applicable for practical application.

Keywords: Unidirectional random waves, High Order Spectral method, the occurrence probability of freak waves, bimodal spectra, quantitative prediction of freak wave occurrence.

1. Introduction

Marine environmental safety has become increasingly important with the rapid development of coastal engineering operations. Freak waves (commonly defined as their wave height exceeding twice the significant wave height) [1], with concentrated energy and strong destructive power, pose a disastrous threat to oceanic engineering and marine equipment. Up to now, the influence of freak waves has not yet been properly incorporated into the relevant design issues, leading to great design defects in marine structures. Therefore, further investigation into the probability of freak waves is important to provide proper guidance for practical engineering.

Notable studies in the statistical characterization of unimodal random waves have been established.

* Corresponding author

E-mail address: zhoubinzhen@scut.edu.cn (B.Z. Zhou)

In 1952, Longuet-Higgins [2] proposed that the wave heights regarded as twice the envelop amplitude obey a Rayleigh probability distribution under the idealized assumption that the process is Gaussian and extremely narrow-banded. However, real water waves in the open are weakly non-linear and with broader spectral bandwidth, resulting in the linear model under-predicts the large wave amplitude especially in severe sea states during typhoons [3][4]. Based on a series of physical experiments, numerical simulations, and theoretical analysis, third-order resonant interactions, known as modulation instability, are believed to be an assignable role in the description of strongly nonlinear wave statistics [5][6][7]. To measure the strength of the interactions in random waves, Janssen [5] defined a parameter named Benjamin-Feir Index (BFI) to evaluate the domination of the wave steepness and the relative spectral bandwidth. The evolution of random waves considering various BFI values was analyzed. They found that the Rayleigh distribution can predict the wave height distribution when BFI is small, but it underestimates the tail of the exceedance probability of wave height distribution for larger BFI values. Several researchers discussed that exceedance probability was associated with kurtosis, defined as the fourth-order moment of the free surface elevation [5][7][8], and pointed out that the tail of the exceedance probability of wave height distribution increases as the kurtosis value increases [9]. Hence, kurtosis is recognized as an indication of extreme events and introduced as a correction of the Rayleigh model to develop a modified Edgeworth-Rayleigh distribution (MER) [7]. Recently, Wang et al. [10] promoted an extensive investigation of the coupled effect of modulational instability and relative water depth and summarized a contour plot of maximum kurtosis considering these two main factors based on a fully nonlinear wave model. Followed by this research, further research on the relation between the occurrence probability of freak waves and kurtosis was conducted by Wang et al. [11]. An empirical formula for unimodal long-crested wave trains was proposed, in which there is a little deviation from the prediction obtained from MER weakly nonlinear model.

The majority of the previous studies are focused on wave configuration under a single-peak spectrum. However, 15%-25% of the actual sea states around the world are observed to be a two-peak structure describing swell and wind-sea mixed systems [12][13]. A more accurate prediction of extreme responses needs to be estimated in such systems. Several exploratory studies have been made in the circumstance of two crossing systems. Onorato et al. [14] found that wider areas of instability occur with a faster growth rate for coupled systems by a theoretical analysis based on nonlinear Schrödinger (CNLS) equations. Regev et al. [15] proposed that a swell-dominated system crossing with a wind-sea-dominated system at a preferred angle can arise extra instability modulations, causing an increased chance of large wave occurrence. Additionally, it was also explored that when a weakly swell-dominated system perturbed a wind-sea-dominated system by oriented at various angles, the occurrence probability of freak waves can be enhanced slightly [16]. Further, Toffoli et al. [17] pointed out that the kurtosis increases with an interaction angle of these two systems between 40 and 60°.

Instead, the statistical characteristics of the co-propagating mixed waves are not yet further understood, unlike the crossing systems. Till now, few studies exist with wave configurations under the assumption of equal significant wave height [18][19] or with the same wind-sea spectrum [20]. Petrova and Guedes Soares [18][19] noticed the effects of the relative energy distribution and observed that the kurtosis in a swell-dominated sea state is smaller compared with that in a wind-sea-dominated sea state. Støle-Hentschel et al. [20] pointed out that the crossing mixed waves have milder extreme event statistics than that of pure wind-sea-dominated waves.

In real sea states, directional properties are proven to have a great impact on statistical characteristics [21]. However, due to facility limitations, it is a common practice in coastal engineering and marine

operations to focus on unidirectional waves [22], especially during model tests. This simplification is also beneficial to evaluating the wave loads in the design of coastal structures. As a result, the wave configuration defined as a unidirectional description has kept the subject of most investigations, involved in this study. Additionally, an extra understanding of co-propagating mixed waves is also important as a limiting case for spreading seas. The wave configuration is often defined by simple integral parameters such as characteristic wave height or characteristic wave period. While, for a bimodal sea state, the energy is divided into the low-frequency part and the high-frequency part. Such a nonlinear interaction process is far more complicated than the linear superposition of two unimodal processes [10] [20]. The possible limitations inherent to the above description need to be investigated by the use of bimodal spectra.

The quantitative indicators of the freak wave occurrence in this mixed physical context are not yet available. Wang et al. [10] extensively summarized the coupled effects of modulational instability and relative water depth in unimodal sea states, and qualitatively analyzed the impacts of *Sea-Swell Energy Ratio* (SSER) and *Intermodal Distance* (ID) in bimodal waves on the statistical properties. Unfortunately, the quantitative relation between the freak wave occurrence probability and the initialized wave parameters is not established. Thus, the objective of our present work is consequently to bridge this gap to provide a more intuitive understanding. The novelties are two-folded. First, the quantitative relation between the occurrence probability of freak waves concerning unidirectional wave configuration under bimodal spectra is established. Second, an empirical formula of the relation between the kurtosis of bimodal waves and that of unimodal sea states is given.

The rest of the paper is arranged as follows. Section 2 defines the bimodal sea state and gives the co-propagating mixed wave configurations. Section 3 describes the set-up of the HOS numerical wave tank and defines relative characteristics in the coming analysis. Section 4 investigates the quantitative relation between the occurrence probability of freak waves and unidirectional wave configuration under bimodal spectra. The empirical formula of the relation between the kurtosis of bimodal waves and that of unimodal sea states is derived, which is rarely seen in previous studies.

2. Co-propagating mixed wave configuration

As an extension of the study by Wang et al. [10], the influence of wave spectral type on the nonlinear statistical characteristics will be further investigated under the assumption of equivalent energy with unimodal wave trains in this work. Unidirectional random wave configurations are commonly characterized by such integral parameters as significant wave height or mean zero-crossing period. Unfortunately, the energy distribution within the mixed system is almost ignored in previous literature, which is a key factor in studying the statistical behavior of the co-propagating mixed sea state [10] [20]. Thus, the quantitative relation of occurrence possibility of freak waves based on a large number of wave configurations including as much spectral distribution as possible should be explored.

2.1 Wave spectrum

Consisting of two systems dominated by different factors, the frequency spectrum $S(\omega)$ proposed by Ochi and Hubble [23] is available for our following study, which has also been adopted by Rodriguez et al. [24][25]. It is illustrated in Fig. 1.

$$S(\omega) = \frac{1}{4} \sum_j \left(\frac{4\lambda_j + 1}{4} \right)^{\lambda_j} \frac{1}{\Gamma(\lambda_j)} \left(\frac{\omega_{pj}}{\omega} \right)^{4\lambda_j} \frac{H_{sj}^2}{\omega} \exp \left[-\frac{4\lambda_j + 1}{4} \left(\frac{\omega_{pj}}{\omega} \right)^4 \right] \quad j = 1, 2 \quad (1)$$

where $j=1, 2$ correspond to the swell-dominated system and wind-sea-dominated system, respectively. Γ is the gamma function. The significant wave height H_s , the angular frequency ω_p ($=2\pi f_p$), and the peak enhancement factor λ are involved to define these two different dominated systems.

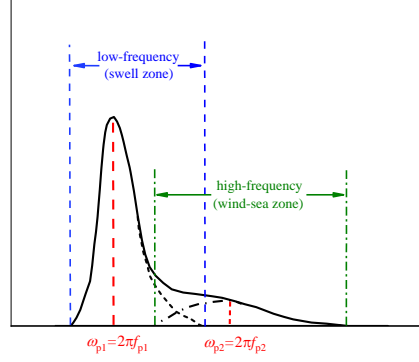


Fig. 1 Schematic diagram of the bimodal spectrum.

The significant wave height H_s of the mixed system can be calculated by the energy superposition according to the Rice theory [26]

$$H_s = \sqrt{H_{s1}^2 + H_{s2}^2} \quad (2)$$

Mean zero-crossing period T_z of the mixed system can be calculated by the energy weighting, expressed as:

$$\sqrt{\frac{H_{s1}^2 + H_{s2}^2}{H_{s1}^2 / T_{z1}^2 + H_{s2}^2 / T_{z2}^2}} = T_z \quad (3)$$

$$T_{z1} = 2\pi \sqrt{\frac{m_{01}}{m_{21}}} \quad T_{z2} = 2\pi \sqrt{\frac{m_{02}}{m_{22}}} \quad (4)$$

where m_{01} and m_{21} are the zero- and second-order spectral moments of the swell-dominated system, and m_{02} and m_{22} are the corresponding spectral moments of the wind-sea-dominated system, respectively.

2.2 Definition of co-propagating mixed waves

There are two dimensionless parameters to help describe the specific property of the bimodal spectral waves.

One describes the energy distribution in the mixed waves, namely *Sea-Swell Energy Ratio* (SSER) [25]. It is defined as an energy ratio, viz. the zero-order spectral moment (m_0) of the wind-sea-dominated system against that of the swell-dominated system, given as:

$$\text{SSER} = \frac{m_{0_{\text{wind-sea}}}}{m_{0_{\text{swell}}}} \quad (5)$$

The configuration with SSER around 1.0 corresponds to a sea state with sea-swell equivalent energy. For SSER smaller than 1.0, the configuration represents a swell-dominated sea state. For a larger SSER

value, it seems a wind-sea-dominated sea state.

Another parameter describes the spectral separation, namely *Intermodal Distance* (ID) [25], expressed as:

$$ID = \frac{f_{p2} - f_{p1}}{f_{p1} + f_{p2}} \quad (6)$$

For a sea state with an ID value close to 0, the peak frequencies of the swell-dominated and wind-sea-dominated systems are in proximity. While for a sea state with an ID value up to 0.10 or larger, the swell-dominated system and the wind-sea-dominated system are well separated in an almost independent frequency band.

2.3 Parameters of co-propagating mixed configuration

The tested cases focused on co-propagating mixed waves considering various SSER and ID values are listed in Tab. 1. Case single-peak, with a moderate value of BFI [5] is taken for comparison. The mean zero-crossing periods T_z in all bimodal cases are consistent with that under the unimodal spectrum. The listed co-propagating mixed configurations represent not only the sea states have various ID values with fixed SSER (Cases A-J) but also the sea states have various SSER values with fixed ID (Cases AA-AE, AF-AJ, AK-AO, and AP-AT). As concluded by Baldock [27], freak waves are more likely to appear in wave trains with a narrower spectrum. Therefore, a study on the occurrence probability of freak waves in the sea state of two wave trains with narrower spectra can obtain a conservative threshold. Considering that the relative spectral bandwidth $\Delta f/f_p$ of the case with enhancement factor $\lambda=16$ in the bimodal spectrum, corresponds to that of the case with $\gamma=7$ in the widely used single-peak JONSWAP spectrum, according to Ref. [10], $\lambda_1=\lambda_2=16$ is adopted in this study. It represents a special state that is close to the upper limit of wind-generated waves [28].

The total energy of the wave trains is associated with the length of the wave trains to be analyzed, which means the more the number of waves, the greater the total energy of the wave trains. Considering that, the amplitude spectrum a_i of each wave component is given here, defined from the wave spectrum from Eq. (1)

$$a_i = \sqrt{2S(\omega_i)\Delta\omega_i} \quad (7)$$

where $\Delta\omega_i=2\pi(f_H-f_L)/(N_f-1)$ represents the division widths of the frequencies. N_f is the total number of the frequency division, adopted as 200 in this study. $(f_L, f_H)=(0.2\text{Hz}, 3.0\text{Hz})$ donates the considered frequency range. To avoid the periodic time repetition of the time series, the typical frequency of the i^{th} wave component ω_i is randomly selected as

$$\omega_i = (i-1 + rand)\Delta\omega_i \quad (8)$$

where *rand* is a random number distributed from 0 to 1.

Fig. 2 illustrates the input amplitude spectra of the co-propagating mixed waves, with a single-peak spectrum as a reference. In Fig. 2a, the ID values vary from 0.02 to 0.20 with the SSER value fixed as 1.0. When the ID value is small (Cases A-C), the amplitude spectra appear in several wide spectral bandwidth structures but have no obvious bimodal characteristic. As the ID value increases up to 0.10 or larger (Cases F-J), the two frequency peaks of the different dominated systems are completely separated, with a clear presence of a double-peak appearance. While in Fig. 2b, the SSER value is variable in each case with the ID fixed as 0.20.

Tab. 1 Detailed parameters of tested cases on co-propagating mixed waves ($h=4.0\text{m}$, $\lambda_1=\lambda_2=16$).

Case	f_p (Hz)	H_s (m)	SSER	ID
single-peak	1.0	0.03	-	-
Case A	0.98	0.0212	1.00	0.02
	1.02	0.0212		
Case B	0.96	0.0212	1.00	0.04
	1.04	0.0212		
Case C	0.94	0.0212	1.00	0.06
	1.06	0.0212		
Case D	0.92	0.0212	1.00	0.08
	1.08	0.0212		
Case E	0.90	0.0212	1.00	0.10
	1.09	0.0212		
Case F	0.84	0.0212	1.00	0.15
	1.14	0.0212		
Case G	0.78	0.0212	1.00	0.20
	1.18	0.0212		
Case H	0.73	0.0212	1.00	0.25
	1.21	0.0212		
Case I	0.67	0.0212	1.00	0.30
	1.25	0.0212		
Case J	0.62	0.0212	1.00	0.35
	1.27	0.0212		
Case AA	0.98	0.0276	0.18	0.06
	1.11	0.0117		
Case AB	0.96	0.0249	0.46	0.06
	1.08	0.0168		
Case AC	0.94	0.0212	1.00	0.06
	1.06	0.0212		
Case AD	0.92	0.0173	2.06	0.06
	1.04	0.0245		
Case AE	0.90	0.0111	6.46	0.06
	1.01	0.0279		
Case AF	0.98	0.0283	0.12	0.08
	1.15	0.0099		
Case AG	0.95	0.0254	0.40	0.08
	1.12	0.0160		
Case AH	0.92	0.0212	1.00	0.08
	1.08	0.0212		
Case AI	0.90	0.0185	1.68	0.08
	1.06	0.0236		
Case AJ	0.88	0.0144	3.44	0.08
	1.03	0.0263		
Case AK	0.98	0.0287	0.09	0.10
	1.20	0.0087		
Case AL	0.94	0.0257	0.37	0.10
	1.15	0.0155		
Case AM	0.90	0.0212	1.00	0.10
	1.10	0.0212		

Case AN	0.88	0.0192	1.49	0.10
	1.08	0.0231		
Case AO	0.85	0.0141	3.66	0.10
	1.04	0.0265		
Case AP	0.95	0.0287	0.09	0.20
	1.43	0.0088		
Case AQ	0.88	0.0263	0.31	0.20
	1.32	0.0145		
Case AR	0.79	0.0212	1.00	0.20
	1.18	0.0212		
Case AS	0.75	0.0184	1.66	0.20
	1.13	0.0237		
Case AT	0.70	0.0123	4.99	0.20
	1.05	0.0274		

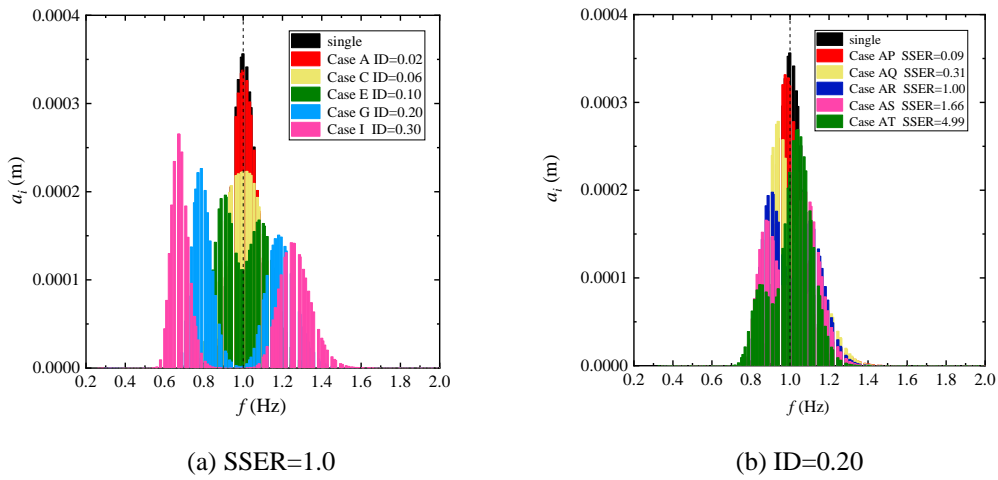


Fig. 2 Input amplitude spectra of tested cases on co-propagating mixed waves considering various ID and SSER values.

3. Numerical set-up and analytical parameters

3.1 Numerical model

Statistical characteristics can be obtained based on time series data from the continuous long-time simulation. In this study, the High Order Spectral (HOS) method is applied to solve the potential flow equations with a great advantage in computing efficiency and accuracy.

Introducing the wavemaker boundary, the numerical wave tank based on the HOS method can be solved with the method of splitting the velocity potential into a sum of two-part potential. One is the free-surface spectral potential component Φ_f , consisting of a perturbation series up to an arbitrary order. The other is the prescribed non-periodic component Φ_w , expressed on another set of specific basis functions concerning a given wave maker boundary. For more details can refer to Ref. [29].

The numerical wave tank adopted to simulate co-propagating mixed waves is shown in Fig. 3, with the fluid at rest as the initial condition. The unidirectional waves are generated at the left side with a time-varying boundary condition. The wave maker's motion depends on the expected free surface elevation and its specific transfer function.

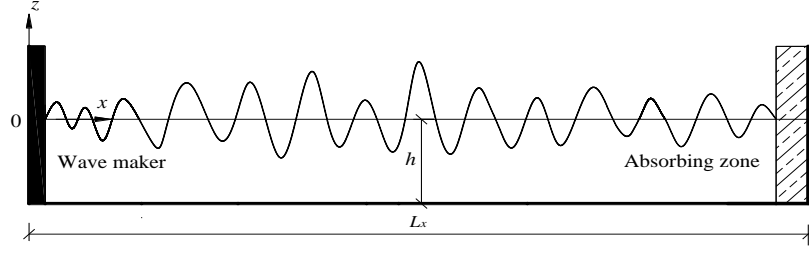


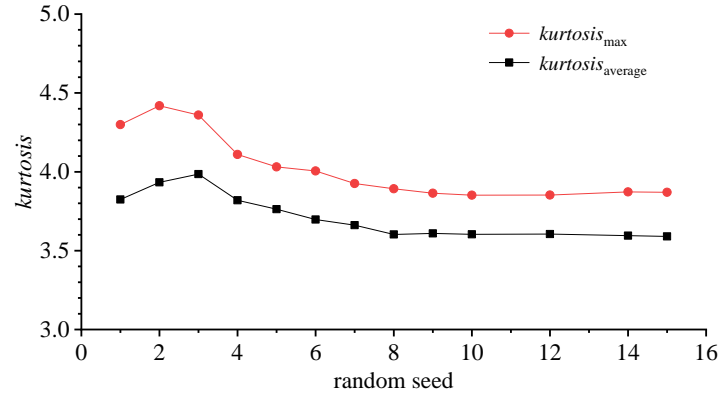
Fig. 3 Sketch of the numerical wave tank including a wave maker and an absorbing zone.

3.2 Numerical set-up

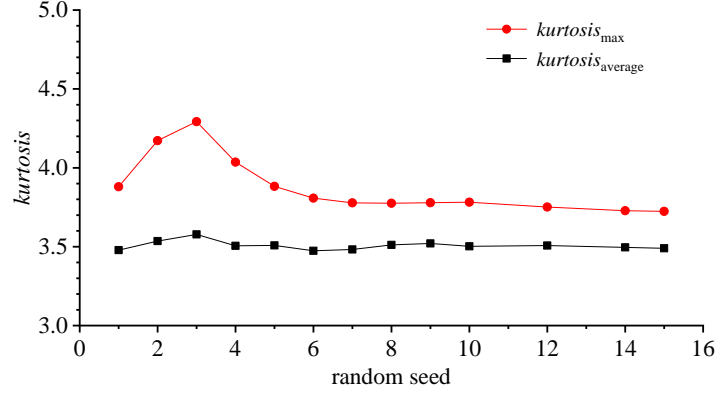
For all tested cases, the total number of wave components is 200 within a frequency range of [0.2Hz, 3.0Hz]. Per peak wavelength is discretized by 30 in space, per wave period is 100 in time step, and the nonlinear order of the HOS method is 5. Convergence analysis and validation have been conducted, referring to Ref. [10].

The numerical wave tank is taken as at least 50 times the target peak wavelength, corresponding to 220m effective length down the direction of the wave propagation, aiming for sufficient evolution in space. The operational water depth is kept at 4.0m throughout the tests. More details on the present implementation and set-up parameters can be referred to in Ref. [10].

Inspired by Moriarty et al. [30], Fig. 4 presents examples of the evolution of the statistical moments for Case single-peak and one of bimodal case (Case A) against the number of random seeds, including the maximum value and the average value of kurtosis along the wave tank. It can be found that 10 random runs are sufficient to obtain a reliable estimate, under the assumption of nearly 1000 times of spectral peak wave period with each random phase.



(a) Case single-peak



(b) Case A

Fig. 4 Evolution of the ensemble-averaged evaluated statistical moments as a function of the number of runs.

During the numerical simulation, a large number of waves needed to be generated and measured for statistics. Ten random seeds different from each other are to be chosen for more universal results. Finally, at least 5000 waves are ensured to be effectively collected by all gauges in each wave configuration.

3.3 Analytical parameters

Statistical parameters of the co-propagating mixed waves, such as kurtosis and wave height distribution, are to be discussed in the following analysis.

3.3.1 Kurtosis

Kurtosis of the time series of free surface elevation is defined as:

$$kurtosis = \frac{\langle (\eta - \langle \eta \rangle)^4 \rangle}{\sigma^4} \quad (9)$$

where $\langle \rangle$ represents the average over time and σ is the standard deviation of free surface elevation η .

3.3.2 Exceedance probability of wave height

(a) Rayleigh distribution

In Rayleigh distribution, the wave height is considered as twice the envelope amplitude in a Gaussian and even narrow-banded process [1]:

$$E(H) = \exp \left[-\frac{H^2}{8m_0} \right] \quad (10)$$

in which $m_0 = (H_s/4)^2$.

(b) MER distribution

Adding the effect of weakly nonlinear interaction between wave components, Mori and Janssen [7] advanced the MER model under the assumption of the narrow spectrum and wave height twice wave amplitude, expressed as:

$$E(H) = \exp \left(-\frac{H^2}{8m_0} \right) \left[1 + (kurtosis - 3) \frac{H^2}{384m_0} \left(\frac{H^2}{m_0} - 16 \right) \right] \quad (11)$$

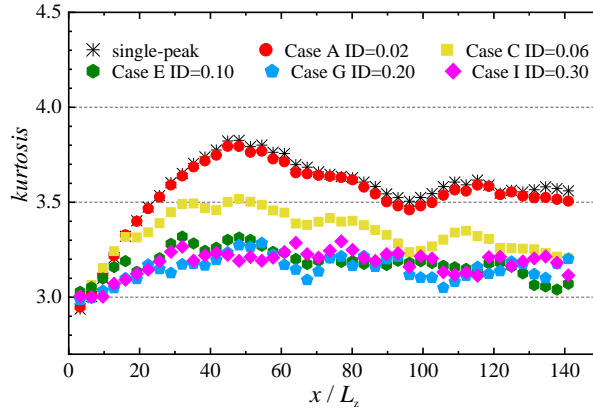
4. Quantitative analysis

4.1 Spatial evolution of kurtosis

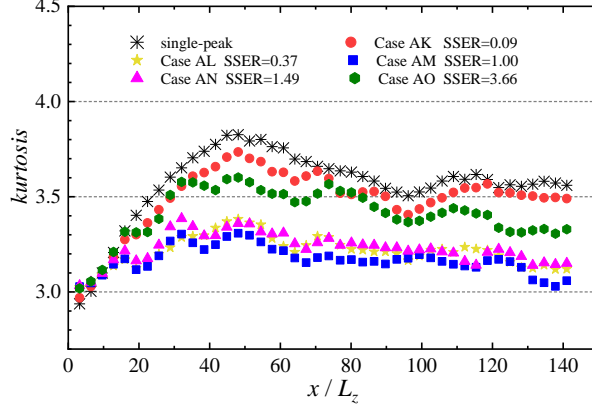
As waves move away from the wave maker, accompanied by the enhancement of the nonlinear interactions between wave components, the parameter associated with increasing freak waves, namely kurtosis, shows different statuses down in the wave propagation direction. Based on our previous study [10], the spatial evolution of kurtosis in bimodal spectral long-crested wave trains is illustrated in Fig. 5 considering a wide range of ID and SSER values. The horizontal axis is uniformly nondimensionalized by the characteristic wavelength L_z corresponding to the mean zero-crossing period.

The value of kurtosis reaches a maximum after the wave train propagates several wave periods. For the sea states with fixed SSER (Fig. 5a), the maximum value of kurtosis gradually increases as the ID value increases. But till the spectral structure appears evident bimodal pattern, viz. ID value larger than 0.10 (Case F-J), the changes of kurtosis down the wave propagation are less significant. Whereas, for the cases with fixed ID (Fig. 5b), when SSER is less than 1.0, kurtosis with a larger SSER tends to have a smaller maximum value. For a wave configuration with SSER=1.0, viz. a sea-swell energy equivalent sea state, kurtosis reaches its minimum value. Subsequently, as SSER continually increases, the kurtosis begins to increase but still less than that corresponding to the single-peak spectral wave states.

Although the statistical characteristics of all different locations down the bimodal spectral wave trains exhibit different kurtosis, it is always smaller than that of the corresponding single-peak spectral wave states irrespective of the values of ID and SSER, under the assumption of equal wave energy.



(a) SSER=1.0



(b) ID=0.10

Fig. 5 Spatial evolution of kurtosis down the wave propagation for tested cases considering various values of ID and SSER in co-propagating mixed waves. The unimodal and bimodal results are marked with black scatters and colorful scatters, respectively, both counted from measured data at 44 gauges placed 5m apart.

4.2 Distribution of maximum kurtosis

As known, for single-peak spectral wave trains, the maximum kurtosis can be deduced by a contour plot with information on the incident wave field involved [10] (such as deep-water BFI and the relative water depth $k_p h$). Nevertheless, for co-propagating mixed waves, the nonlinear interaction process is closely associated with the energy distribution within the mixed system. This leads to a more complex maximum kurtosis profile than that of the unimodal system with additional parameters to consider. As such, in this study, we explore the relation of the maximum kurtosis between single-peak and bimodal wave trains with equivalent energy, by introducing energy distribution SSER and frequency separation ID.

In Ref. [10], the variation of the maximum kurtosis with various ID values in co-propagating sea-swell energy equivalent wave configuration is given, shown in Fig. 6. It presents the maximum value of kurtosis down the wave propagation versus ID in co-propagating sea-swell energy equivalent wave configuration. When the ID value is smaller than 0.10, the maximum kurtosis decreases with the increase of ID with a trend of rapid decline at first and then followed by a tendency towards a steady state. While, for cases with an ID value larger than 0.10, the maximum kurtosis is constant at around 3.3 almost with no change. Besides, Fig. 6 also gives a regression relation, in which the trend is applicable to be fitted by the Boltzmann model, and the regression curve can be obtained as follows

$$kurtosis_{\max-\text{bimodal}} = 3.29 + \frac{kurtosis_{\max-\text{single}} - 3.29}{1 + \exp[100(\text{ID} - 0.056)]} \quad (\text{SSER} = 1.0) \quad (12)$$

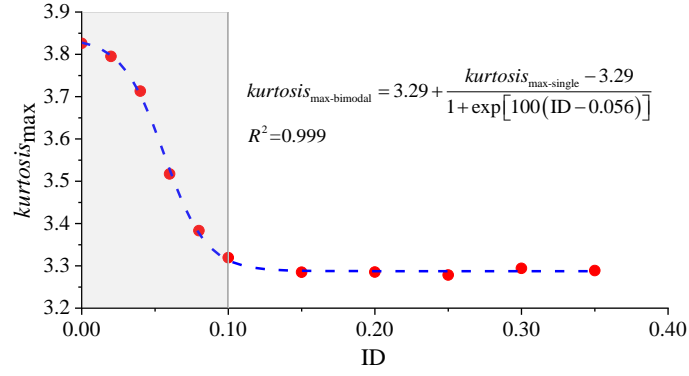


Fig. 6 Influence of ID value on maximum kurtosis in co-propagating sea-swell energy equivalent wave configuration (SSER=1.0).

In Ref. [10], the influence of SSER values on maximum kurtosis values in various co-propagating mixed sea states is given, here shown in Fig. 7. For a swell-dominated wave condition (*i.e.*, SSER<1.0), the maximum value of kurtosis decreases greatly with the increase of SSER value. Thereafter, for a wave condition with an SSER value larger than 1.0 (*i.e.*, wind-sea-dominated wave condition), the maximum kurtosis gradually increases as the SSER value increases. That is, in swell-dominated or wind-sea-dominated sea states, the statistical maximum values of kurtosis are larger than that of the configuration in sea-swell energy equivalent sea state but smaller than that of the case in unimodal spectral waves. Based on this, here we observe that for cases with various ID values, a bi-Gaussian fit is applied to predict the maximum kurtosis value. The fitting relation obtained from Fig. 7 is expressed as

$$kurtosis_{\max-bimodal} = \begin{cases} kurtosis_{\max-single} + a * \exp\left[-\frac{(SSER-1.0)^2}{0.98}\right] & SSER < 1.0 \\ kurtosis_{\max-single} + a * \exp\left[-\frac{(SSER-1.0)^2}{9.68}\right] & SSER \geq 1.0 \end{cases} \quad (13)$$

where a is the maximum kurtosis value in sea-swell energy equivalent sea state, which can be obtained from Eq. (12).

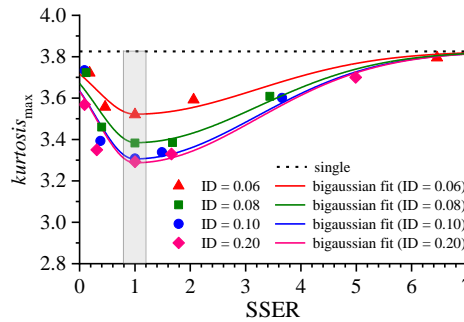


Fig. 7 Influence of SSER values on maximum kurtosis values in co-propagating mixed waves. The horizontal black dotted line represents the maximum kurtosis of the corresponding wave trains under the single-peak spectrum. The scattered points in the shaded area represent the maximum kurtosis in sea-swell energy equivalent wave configuration (SSER=1.0), part of Fig.5.

The comparison between statistical data and fitting results of the maximum kurtosis with various ID and SSER values is given in Fig. 8. Most of the data are scattered near the uphill straight-line $y=x$. This indicates that either the Boltzmann fit or the bi-Gaussian fit has high accuracy in predicting maximum

kurtosis values with various ID and SSER values in bimodal spectral unidirectional wave trains.

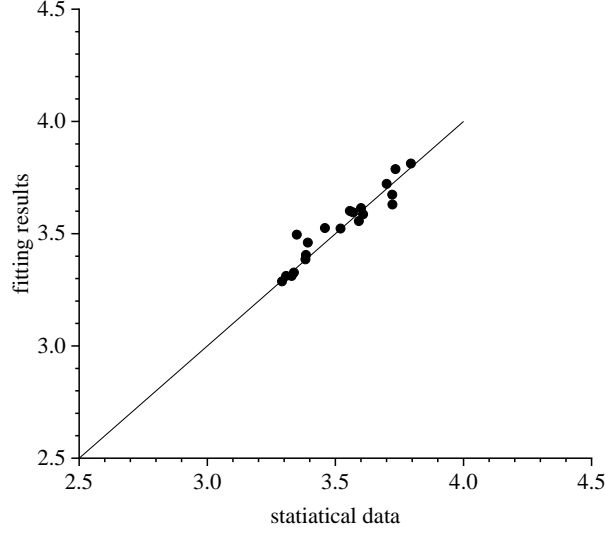


Fig. 8 Comparison of statistical data and fitting results based on the combination of Boltzmann fit and bi-Gaussian fit.

4.3 Exceedance probability of wave height at maximum kurtosis

Wave height distribution is an important method to analyze the occurrence probability of freak waves [6][7][9] when we adopt the definition of freak waves as the waves with the wave height twice of the significant wave height. Kurtosis is regarded as a measure closely correlated with the probability of large waves. The larger the kurtosis value, the larger the deviation from the Rayleigh distribution, and the greater the probability of freak waves. Some theoretical models existing for predicting the wave height distribution, such as the Rayleigh distribution or MER distribution mentioned above, are under the linear hypothesis or the weakly nonlinear hypothesis. However, for broader spectral unidirectional wave trains (for instance, co-propagating mixed waves focused in this study), there is indeed rare research concerned about the specific quantitative relation between these two. Thus, Further research is needed to explore the effectiveness of the existing wave height distribution model for predicting the occurrence probability of freak waves in bimodal wave configuration.

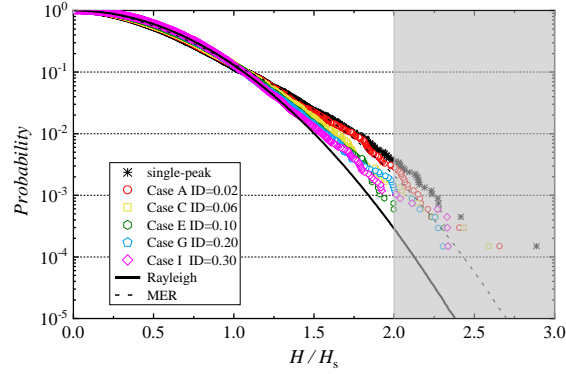
The exceedance wave height distribution at the position where kurtosis achieves the maximum value is given in Fig. 9, with Rayleigh and MER theoretical distribution of the corresponding single-peak spectral waves as reference. In the figure, the shaded area represents H/H_s greater than 2.0, which is commonly adapted for the definition of the freak wave. The probability corresponding to the threshold (i.e., $H/H_s=2.0$) is used to define the occurrence probability of freak waves P_{freak} in this study.

Similar to the phenomena observed in single-peak spectral waves [11], Rayleigh distribution underestimates the statistical wave height when $H/H_s \geq 2.0$ in all bimodal wave configurations. For the wave configuration with fixed SSER (Fig. 9a), the deviation from Rayleigh distribution becomes gradually smaller as ID becomes larger. Till the swell partition and the wind-sea partition are completely separated (Case G ID=0.20 and Case I ID=0.30), the statistical wave height is close to the Rayleigh distribution. Meanwhile, for the cases with smaller ID values (Case A ID=0.02 and Case C ID=0.06), MER distribution can well predict the statistical wave height. While, for the wave states with larger ID values (Cases E-I ID=0.10-0.30), MER distribution overestimates the statistical wave height, and the deviation from MER distribution gradually increases with the increase of ID.

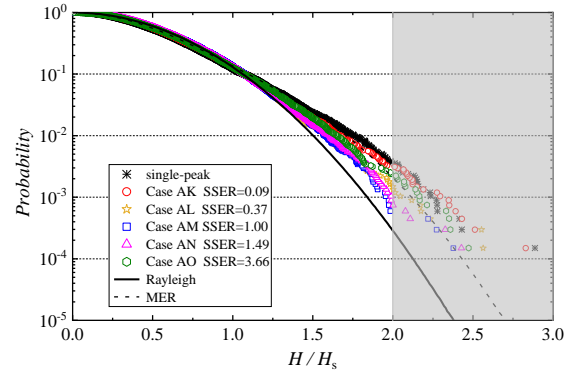
Whereas, for the wave configuration with fixed ID (Fig. 9b), when SSER is less than 1.0 (i.e.,

swell-dominated sea state), statistical wave height with a larger SSER has a smaller deviation. Till SSER reaches 1.0, deviation from Rayleigh distribution is insignificant. Subsequently, as SSER continues increasing (i.e., wind-sea-dominated sea state), the deviation from Rayleigh distribution becomes gradually larger but still less than that corresponding to the single-peak wave configuration. Additionally, the statistical wave height of the wave configuration with various SSER values deviates from MER distribution on both sides, and the largest deviation occurs in the wave configurations under unimodal spectrum and with SSER=1.0.

From the above analysis, both two conventional prediction theoretical models, neither Rayleigh distribution nor MER distribution, could predict the statistical wave height in bimodal wave configuration, especially for the occurrence probability of freak waves.



(a) SSER=1.0



(b) ID=0.10

Fig. 9 Exceedance probability of wave height at maximum kurtosis for various ID and SSER values in co-propagating mixed waves. Both Rayleigh distribution (black solid line) and MER distribution (black dotted line) for reference are obtained based on the corresponding single-peak spectral waves.

4.4 Empirical relation between occurrence probability of freak waves and kurtosis

Based on the exceedance wave height distribution at maximum kurtosis above, the occurrence probability of freak waves, that is the probability when $H/H_s=2.0$, in wave configuration with various ID and SSER values can be extracted. The variation of the occurrence probability of freak waves with kurtosis can be investigated, shown in Fig. 10. Oblique black solid lines give the results from regression analysis, and black dotted lines give the upper and lower boundary of the 95% prediction band.

In Fig. 10a, with a fixed SSER value, the maximum kurtosis, as well as the maximum freak wave

occurrence probability P_{freak} , gradually decreases as the ID value increases. In Fig. 10b-e, when the ID value is constant, for a swell-dominated sea state (i.e., $SSER < 1.0$), the maximum value of kurtosis and the maximum freak wave occurrence probability P_{freak} synchronous decreases as SSER increases up to 1.0. Then, for a wind-sea-dominated sea state (i.e., $SSER > 1.0$), the maximum value of kurtosis and the maximum freak wave occurrence probability P_{freak} increase with the increase of SSER value. The occurrence probability of freak waves P_{freak} has a positive linear correlation with kurtosis under these circumstances.

Further, for the wave configuration with different intermodal distances ID, the slope of the freak wave occurrence probability P_{freak} against kurtosis remains almost unchanged, also consistent with that obtained in sea-swell energy equivalent wave configuration. This means that the relation between the occurrence probability of freak waves and kurtosis is hardly affected by the ID and SSER values.

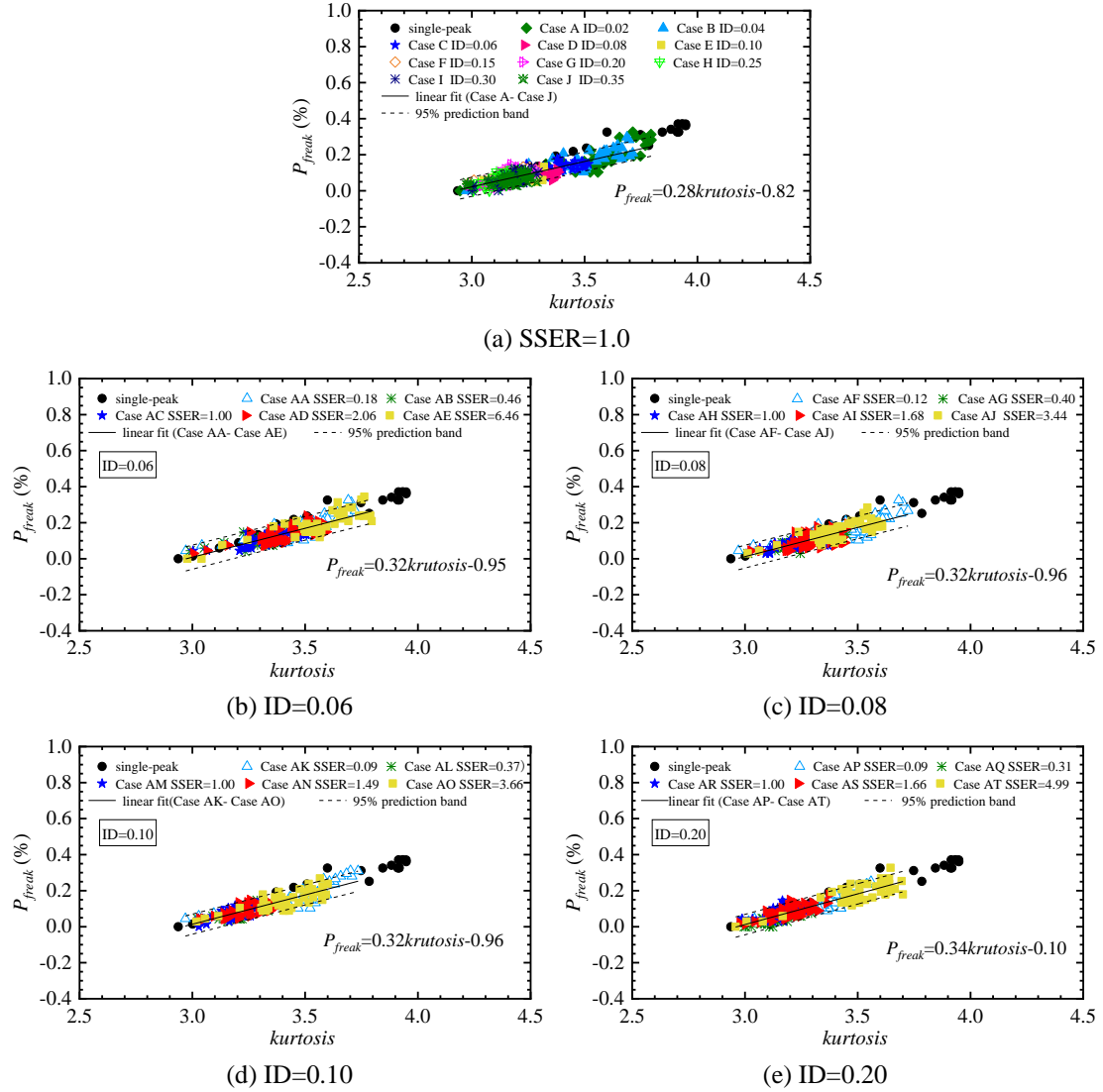


Fig. 10 Variation of occurrence probability of freak waves with kurtosis considering various ID and SSER values in co-propagating mixed waves.

In general, the empirical formula reflecting the relation between the occurrence probability of freak waves P_{freak} and kurtosis in co-propagating mixed waves is shown in Fig. 11. Statistical properties exhibited in different locations down the wave propagation are covered. It can be observed that there is a uniform positive linear correlation between the occurrence probability of freak waves P_{freak} and

kurtosis, irrespective of intermodal distances ID and energy distribution SSER. This is quite consistent with the previous observations in the single-peak spectral wave conditions. That is, when the kurtosis value is larger, the statistical value of the occurrence probability of freak waves is a little larger than the prediction from MER and much larger than that from Rayleigh. These differences cannot be ignored in the design stage of coastal engineering structures. The empirical formula is expressed as

$$P_{freak} = 0.29kurtosis - 0.82 \quad (14)$$

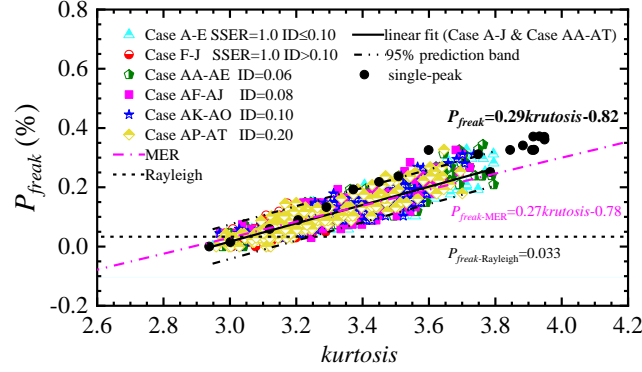


Fig. 11 Relation between occurrence probability of freak wave and kurtosis for all tested cases considering various ID and SSER values in co-propagating mixed waves.

Therefore, once given the integral parameters (the mean zero-crossing period T_z) of the wave configuration and the input spectral distribution (intermodal distances ID and energy distribution SSER), maximum kurtosis in bimodal waves can be predicted by Eqs. (13) and (12), with the help of the previously established relation between maximum kurtosis and wave field parameter under single-peak spectrum by Wang et al. [10]. And then bringing into the empirical relation between the occurrence probability of freak waves and kurtosis (Eq. (14)), the occurrence probability of freak waves in this wave configuration can be predicted. Thus, it can be realized that for a given bimodal wave configuration, the occurrence probability of freak waves in operational conditions can be quickly predicted. This prediction method provides a valuable reference for practical engineering such as the site selection of coastal projects or the load design of marine structures.

5. Conclusions and discussions

In this paper, the occurrence probability of freak waves in unidirectional waves under bimodal spectra is predicted, based on continuous long-time simulated data considering full nonlinearities in the High Order Spectral (HOS) numerical wave tank.

The effects of the wave spectral type on the statistical characteristics are investigated in co-propagating mixed waves with equivalent energy. Compared with the results from the unimodal cases, the maximum value of kurtosis and wave height distribution under the bimodal spectrum is smaller than that under the unimodal spectrum. This phenomenon reflects that the wave configuration defined by co-propagating mixed waves is less likely to contain freak waves. Although the classical unimodal configuration is conservative, addressing the fact that 15% to 25% of the actual wave configurations are mixed systems, a more accurate prediction of extreme events and responses in bimodal waves are required to be evaluated.

For co-propagating mixed waves, the energy is divided into the low-frequency part (corresponding to a swell-dominated system) and the high-frequency part (corresponding to a wind-sea-dominated

system). Such a nonlinear interaction process is far more complicated than the linear superposition of two unimodal processes. The definition of marine conditions by simple integral parameters such as the mean zero-crossing period (T_z) is limited. The relation of the maximum kurtosis between single-peak and bimodal wave trains with fixed integral parameters by introducing *Sea-Swell Energy Ratio* (SSER) and *Intermodal Distance* (ID) is obtained with an empirical formula for the relation between the kurtosis of bimodal waves and that of unimodal sea states.

We find that neither the Rayleigh distribution nor MER distribution, two conventional prediction theoretical models, could predict the wave height statistics in bimodal wave configuration accurately, especially for the occurrence probability of freak waves. The quantitative relation between the occurrence probability of freak waves and kurtosis in unidirectional waves under bimodal spectra is established based on the statistical data.

Thus, with the help of the characteristic relation between maximum kurtosis and wave field parameters under the single-peak spectrum, the occurrence probability of freak waves in the operational area can be quickly predicted at a given bimodal wave configuration. Note that, the prediction model is proposed based on the Ochi-Hubble spectrum. If another bimodal spectrum is used, such as Torsethaugen spectrum [31], whether this empirical formula is suitable should be verified using the idea of the established method in this study.

There may be some limitations of our prediction model due to the assumption of the numerical simulation, such as a wave field considering a given spectral type with one fixed total energy. Additionally, when using a special state that is close to the upper limit of wind-generated waves, the threshold proposed in this paper is a conservative estimate. However, the occurrence probability of freak waves is hardly considered in the general specification in the field of ocean engineering. When it comes to the site selection of offshore engineering and the planning of ship routes, the existing specifications underestimate the extreme circumstances, which will cause serious catastrophic destruction. On one hand, the conclusions of this paper proposed under an extreme sea state can provide a conservative reference threshold for offshore engineering and ship navigation. That is, the occurrence probability of large waves can be quickly predicted according to the wave parameters of the operational wave field. On the other hand, seeking a universal result in the following work is of vital importance for practical application. The work in this paper can provide ideas and methods for the next investigation. That is, the predictions under other different assumptions can be conducted by following this idea.

Acknowledgments

This work is supported by the National Natural Science Foundation of China (52071096), the National Natural Science Foundation of China National Outstanding Youth Science Fund Project (52222109), Guangdong Basic and Applied Basic Research Foundation (2022B1515020036), the Fundamental Research Funds for the Central Universities (2022ZYGXZR014), and EPSRC (EP/V050079/1).

References

- [1] Kharif C, Pelinovsky E. Physical mechanisms of the rogue wave phenomenon. *European Journal of Mechanics - B/Fluids*. 2003; 22(6):603-634.
- [2] Longuet-Higgins MS. On the statistical distribution of the heights of sea waves. *Journal of Marine Research*. 1952; 11:245-266.

- [3] Tayfun MA. Distribution of crest-to-trough wave heights. *Journal of Waterway, Port, Coastal and Ocean Engineering*. 1981;107(3):149-158.
- [4] Stansell P. Distributions of freak wave heights measured in the North Sea. *Applied Ocean Research*. 2004; 26(1-2):35-48.
- [5] Janssen PAEM. Nonlinear four-wave interactions and freak waves. *Journal of Physical Oceanography*. 2003; 33(4):863-884.
- [6] Onorato M, Osborne AR, Serio M, Cavaleri L, Brandini C, Stansberg CT. Observation of strongly non-Gaussian statistics for random sea surface gravity waves in wave flume experiments. *Physical Review E*. 2004; 70(6): 067302.
- [7] Mori N, Janssen PAEM. On kurtosis and occurrence probability of freak waves. *Journal of Physical Oceanography*. 2006; 36(7):1471-1483.
- [8] Mori N, Yasuda T. A weakly non-Gaussian model of wave height distribution for random wave train. *Ocean Engineering*. 2002; 29(10):1219-1231.
- [9] Mori N, Onorato M, Janssen PAEM, Osborne AR, Serio M. On the extreme statistics of long-crested deep water waves: theory and experiments. *Journal of Geophysical Research*. 2007; 112(C9):C09011.
- [10] Wang L, Li J, Liu S, Ducrozet G. Statistics of long-crested extreme waves in single and mixed sea states. *Ocean Dynamics*. 2021; 71: 21–42.
- [11] Wang L, Zhou B, Jin P, Li J, Liu S, Ducrozet G. Relation between occurrence probability of freak waves and kurtosis/skewness in unidirectional wave trains under single-peak spectra. *Ocean Engineering*. 2022; 248(15):110813.
- [12] Guedes Soares C. Representation of double-peaked sea wave spectra. *Ocean Engineering*. 1984; 11(2):185–207.
- [13] Guedes Soares C. On the occurrence of double peaked wave spectra. *Ocean Engineering*. 1991; 18(1-2):167–171.
- [14] Onorato M, Osborne AR, Serio M. Modulational instability in crossing sea states: a possible mechanism for the formation of freak waves. *Physical Review Letters*. 2006; 96(1):014503.1-014503.4.
- [15] Regev A, Agnon Y, Stiassnie M, Gramstad O. Sea-swell interaction as a mechanism for the generation of freak waves. *Physics of Fluids*. 2008; 20(11):112102.
- [16] Gramstad O, Trulsen K. Can swell increase the number of freak waves in a wind-sea? *Journal of Fluid Mechanics*. 2010; 650:57–79.
- [17] Toffoli A, Bitner-Gregersen EM, Osborne AR, Serio M, Monbaliu J, Onorato M. Extreme waves in random crossing seas: laboratory experiments and numerical simulations. *Geophysical Research Letters*. 2011; 38:L06605.
- [18] Petrova PG, Guedes Soares C. Probability distributions of wave heights in bimodal seas in an offshore basin. *Applied Ocean Research*. 2009; 31(2):90–100.
- [19] Petrova PG, Guedes Soares C. Wave height distributions in bimodal sea states from offshore basins. *Ocean Engineering*. 2011; 38(4):658–672.
- [20] Støle-Hentschel S, Trulsen K, Nieto Borge JC, Olluri S. Extreme wave statistics in combined and partitioned windsea and swell. *Water Waves*. 2020; 2:169-184.
- [21] Onorato M, Cavaleri L, Fouques S, Gramstad O, Janssen PAEM, Monbaliu J, Osborne AR, Pakozdi C, Serio M, Stansberg C, Toffoli A, Trulsen K. Statistical properties of mechanically generated surface gravity waves: a laboratory experiment in a three-dimensional wave basin.

Journal of Fluid Mechanics. 2009; 627:235–257.

- [22] Tang T, Adcock TAA. The influence of finite depth on the evolution of extreme wave statistics in numerical wave tanks. *Coastal Engineering*. 2021; 166:103870.
- [23] Ochi M, Hubble E. Six parameter wave spectra. *15th International Conference on Coastal Engineering*. Honolulu, Hawaii, United States. 1976.
- [24] Rodriguez GR, Guedes Soares C, Ferrer L. Wave group statistics of numerically simulated mixed sea states. *Journal of Offshore Mechanics and Arctic Engineering*. 2000; 122(4):282-8.
- [25] Rodriguez G, Guedes Soares C, Pacheco M, et al. Wave height distribution in mixed sea states. *Journal of Offshore Mechanics and Arctic Engineering*. 2002; 124:34-40.
- [26] Rice SO. Mathematical analysis of random noise. *Bell Systems Technical Journal*. 1944; 23(3):282-332.
- [27] Baldock TE. Nonlinear transient water waves. University of London, London. 1996.
- [28] Ochi MK. Ocean waves: the stochastic approach. Cambridge University Press. 1998.
- [29] Li J, Liu S. Focused wave properties based on a high order spectral method with a non-periodic boundary. *China Ocean Engineering*. 2015; 29(1):1-16.
- [30] Moriarty PJ, Holly WE, Butterfield S. Probabilistic methods for predicting wind turbine design loads. *Proceedings of the ASME 2003 Wind Energy Symposium. ASME 2003 Wind Energy Symposium*. Reno, Nevada, USA. January 6–9, 2003; 235-243.
- [31] Torsethaugen K, Haver S. Simplified double peak spectral model for ocean waves. *The 14th International Offshore and Polar Engineering Conference*. Toulon, France, May, 2004; ISOPE-I-04-289.